In: Proc. of the IEEE Int. Conf. on Image Processing (ICIP), pp. 333-336, IEEE Signal Proc. Soc., 2006

IMAGE REGISTRATION OF DIFFERENTLY STAINED HISTOLOGICAL SECTIONS

Jens-Peer Kuska[*], *Ulf-Dietrich Braumann*[*], *Nico Scherf*[*], *Markus Löffler*[*], *Jens Einenkel*[†], *Michael Höckel*[†], *Lars-Christian Horn*[‡]

University Leipzig
Fed. Rep. of Germany

Nicolas Wentzensen[§], *Magnus von Knebel Doeberitz*[§]

University Heidelberg
Fed. Rep. of Germany

ABSTRACT

We have focused our interest on the registration of brightfield transmitted light microscopy images with respect to different histological stainings. For this kind of registration problem we have developed a new segmentation procedure. Based on the obtained *consistent segmentations*, a nonlinear registration transformation is computed. The applied registration procedure uses a curvature-based nonlinear partial differential equation in order to find the appropriate mapping between the images. We present an example for the registration of images of two consecutive histological sections from a uterine cervix specimen, where one section stained with $p16^{INK4a}$ was mapped onto another with H&E staining. Finally, we give an illustrative example for a tissue volume reconstruction based on an alternately stained large serial section.

Index Terms— Biomedical image processing, Biological tissues, Image segmentation, Image color analysis, Image texture analysis, Image registration, Nonlinear differential equations, Partial differential equations

1. INTRODUCTION

Different staining of consecutive tissue sections can provide a valuable amount of additional information about the structure and position of different types of tissues. Especially the combined use of different immunohistochemical staining will facilitate new insights into the interaction of cancer, inflammation and healthy cells in the human body. Multiple- or even double-staining techniques using different immunohistochemical stains applied on *one and the same* section is difficult due to the interaction of the staining agents, and in many cases is not feasible. One solution for that problem might be the usage of consecutive sections, while the application of different staining protocols is accomplished on separate slices.

What basically makes the registration of images of such sections difficult is the partial loss of spatial correspondences between the two sections. The reasons for the deformation between consecutive sections are not only some differences concerning the mechanical stress applied during the preparation, especially while sectioning. The aggressive chemical substances used for the staining usually cause some individual, nonuniform shrinkage of the different tissue types which may be comprised within a certain section. To reconstruct the spatial correspondences between the individual sections the usage of a basically nonlinear registration procedure is required, whereas for the latter we consider a nonparametric partial differential equation approach. However, the registration of differently stained images is not at all straightforward, due to the fact that different stainings may have totally different distributions both in color as well in spatial location. So the direct usage of the color images for the registration process is not possible. This is why we need to accomplish a segmentation step prior to the actual registration which, however, requires the utmost possible consistency referring to the various applied stainings. We consider this intermediate step essential in order to obtain the optimum accuracy for the respective registration transformation. Having done the segmentations at this point, there is no further need to segment after the subsequent registrations, as otherwise would be required in order to do quantitative analyses on the registered data.

2. SEGMENTATION

The segmentation step plays the central role in the registration of slices with different coloring. We focus our interest on the statistical description of the distribution of pixel properties in a d-dimensional feature space. Every staining has an individual distribution in the used color space. We operate in the *RGB* space, but other color spaces may be chosen as well. The identification of different tissue types does not only include pixel differences within the color space. The statistical properties of a pixel's neighborhood may also be important [1, 2, 3]. To include these properties into the segmentation, we construct a d-dimensional vector from selected statistical properties of the pixel, see Figure 1. The neighborhood is included in the segmentation vector using properties such as the color mean value and by the construction of successively

[*]Interdisciplinary Center for Bioinformatics
[†]Dept. of Gynecology and Obstetrics
[‡]Working Group Gynecopathology, Inst. of Pathology
[§]Div. for Applied Tumor Biology, Inst. of Pathology

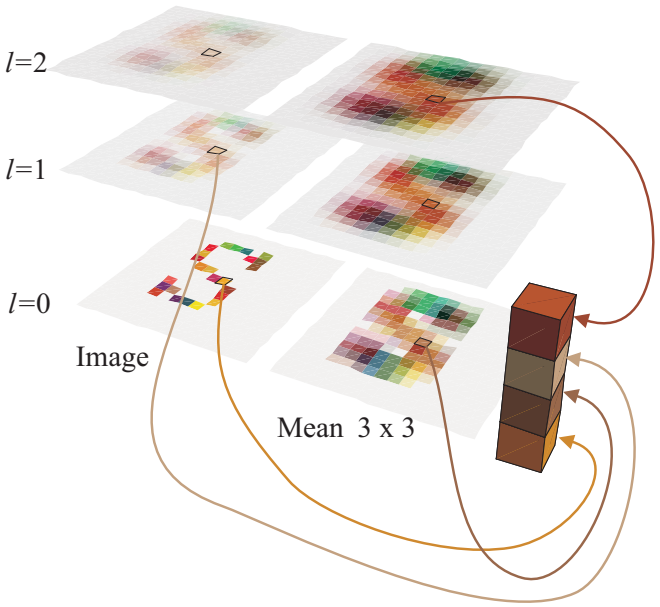

Fig. 1. Construction of the segmentation vector from the color, the mean and the smoothing levels. In this example the segmentation vector is constructed from both the color of the original image and the Gaussian smoothed image, then the mean value of the unsmoothed and the two times smoothed image, giving a 3×4 dimensional segmentation vector.

smoothed images (denoted with the level index l in Figure 1). Frequency properties of the respective pixel are included via sampling along an Archimedean spiral, starting at the respective pixel and analyzing the frequency distribution of a one-dimensional Fourier transform.

The segmentation vectors $\vec{y}_i$ are used to estimate the distribution

$$P(\vec{y}) = \sum_{k=1}^{K} \alpha_k \, p(\vec{y}|\vec{\mu}_k, \Sigma_k) \tag{1}$$

as a linear combination of normal distributions

$$p(\vec{y}|\vec{\mu}, \Sigma) = \frac{(2\pi)^{-d/2}}{\sqrt{\det \Sigma}} \exp\left(-\frac{1}{2}(\vec{y} - \vec{\mu})^T \cdot \Sigma^{-1} \cdot (\vec{y} - \vec{\mu})\right). \tag{2}$$

The estimation of the parameters μ_k, Σ_k and α_k is done using the expectation maximization algorithm [4, 5]. Using the estimated distribution $P(\vec{y})$ we assign every pixel in the image a class number

$$\arg\max_k \frac{\alpha_k \, p(\vec{x}|\vec{\mu}_k, \Sigma_k)}{\sum_{k=1}^{K} \alpha_k \, p(\vec{x}|\vec{\mu}_i, \Sigma_i)} \tag{3}$$

to obtain the image segmentation.

For the two slices with different staining we obtain two segmented images S and S', whereas the class labels assigned by the algorithm must be made *consistent* between the two segmentations. This means, that the labels in one of the segmentations, say S', must be exchanged to match the same regions as in the image S. The segmentation S' may have more classes K' than the segmentation S with K classes. This could occur, for instance, when the second staining marks vessels that cannot be identified in the first staining. In such a case, the class labels must be merged to describe the same region in both segmentations. Merging of two or more classes is also required if an accurate approximation of the density distribution in color space would necessitate a superposition of several single multivariate normal distributions to describe the staining of *one* certain tissue type.

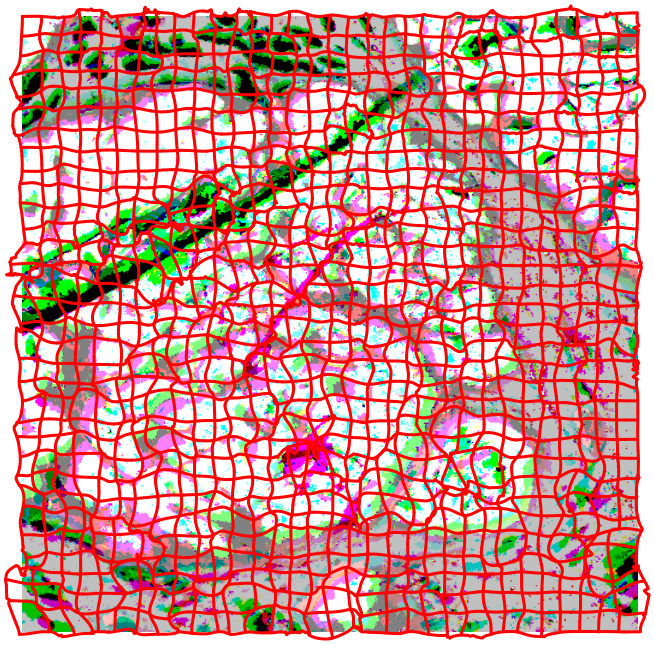

Fig. 2. Displacement field (red lines) obtained by the registration of the segmentations (see Figure 3) of a $p16^{INK4a}$ image (green channel) onto a H&E stained image (red channel) with the transformed segmentation (blue channel). Gray-valued regions are where pair-wise segmentations are consistent both before and after the registrations. Visible combination colors basically occur for the following reasons: Magenta and green margins denote regions where the $p16^{INK4a}$ image was successfully aligned with the H&E image. A few cyan and reddish sites can be found where the $p16^{INK4a}$ image failed to perfectly match with H&E. Yellow sites would mean that a mismatch would have been introduced by the transformation, but such regions practically do not occur.

3. REGISTRATION

From the segmentation we obtain two images with the scalar class label information. These two scalar images are used to compute the displacement field $\vec{u}(\vec{x})$ for the registration. The computation of the displacement field $\vec{u}$ bases on the partial differential equation

$$\alpha \, \Delta^2 \vec{u} - \vec{f}(\vec{x}, \vec{u}) = 0 \tag{4}$$

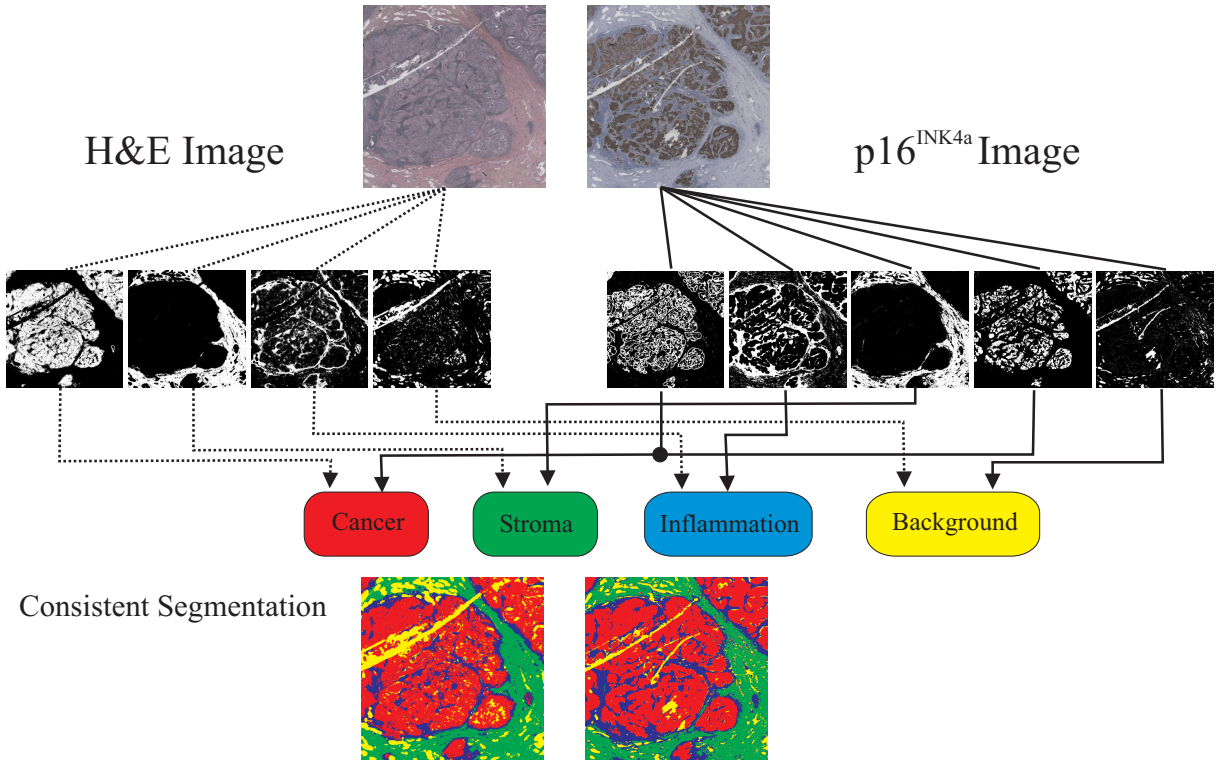

Fig. 3. Principle of the label exchange and label merging (black circle) to obtain a consistent segmentation with four classes for a H&E and p16$^{\text{INK4a}}$ stained image pair. Visible striations are artifacts and occur due to tiny nicks on the microtome blade.

with

$$\vec{f}(\vec{x}, \vec{u}) = \left[S'(\vec{x}) - S(\vec{x} - \vec{u}(\vec{x}))\right] \nabla S(\vec{x} - \vec{u}(\vec{x})) \quad . \tag{5}$$

This equation was introduced in [6][1] and recently studied in [7], wherein Δ denotes the two-dimensional Laplace operator. To allow a smooth convergence for the solution, we introduce an artificial time t and solve the equation

$$\frac{\partial \vec{u}}{\partial t}(\vec{x}, t) + \alpha\, \Delta^2 \vec{u}(\vec{x}, t) = \vec{f}(\vec{x}, \vec{u}(\vec{x}, t)) \quad . \tag{6}$$

The time discretization is done by an implicit midpoint rule and the dependence on the position coordinate $\vec{x}$ in the finite difference approximation of Δ^2 is resolved using a discrete cosine transform. A detailed description about the solution procedure and the used finite difference approximations can be found in [8]. Finally, when the displacement field for the registration is found (see Figure 2 for an illustrative example), the original color image is transformed according to this displacement field to finally obtain the registered version of the original data.

[1]The equation in [6] uses a regularized form of the Laplacian $(\Delta + \epsilon)$ instead of Δ to avoid the division by zero in the inverse operator.

4. EXAMPLE

As an example for the process outlined above, we consider two images with H&E and p16$^{\text{INK4a}}$ staining that should be registered. The tissue types that appear in both images are cancer, inflammation, healthy stroma, and additionally the background. This suggests a total of four classes for the segmentation. For the segmentation of the H&E image we use two smoothing levels and choose the color, the mean value in a 7×7 neighborhood of level $l = 0$ and the slope of the frequency distribution from the first smoothing level. The p16$^{\text{INK4a}}$ image is segmented using the color of level $l = 0$ and the color from the first smoothing level. For the p16$^{\text{INK4a}}$ image we need an additional normal distribution to describe the color of the cancer region. We end up with four classes for the H&E image, and five classes for the p16$^{\text{INK4a}}$ staining. The colors labels of the p16$^{\text{INK4a}}$ segmentation were reordered, and the two classes for the cancer region were merged (see Figure 3 for the summary of the operations). The *consistent segmentations* obtained by these operations were used to compute the displacement field and were further applied to the original p16$^{\text{INK4a}}$ stained image. The result of this operation can be seen in Figure 2. To outline the quality of the image registration obtained by the proposed method we show the result for an alternating sequence of H&E and p16$^{\text{INK4a}}$ stained images. The consistent segmentation of every slice

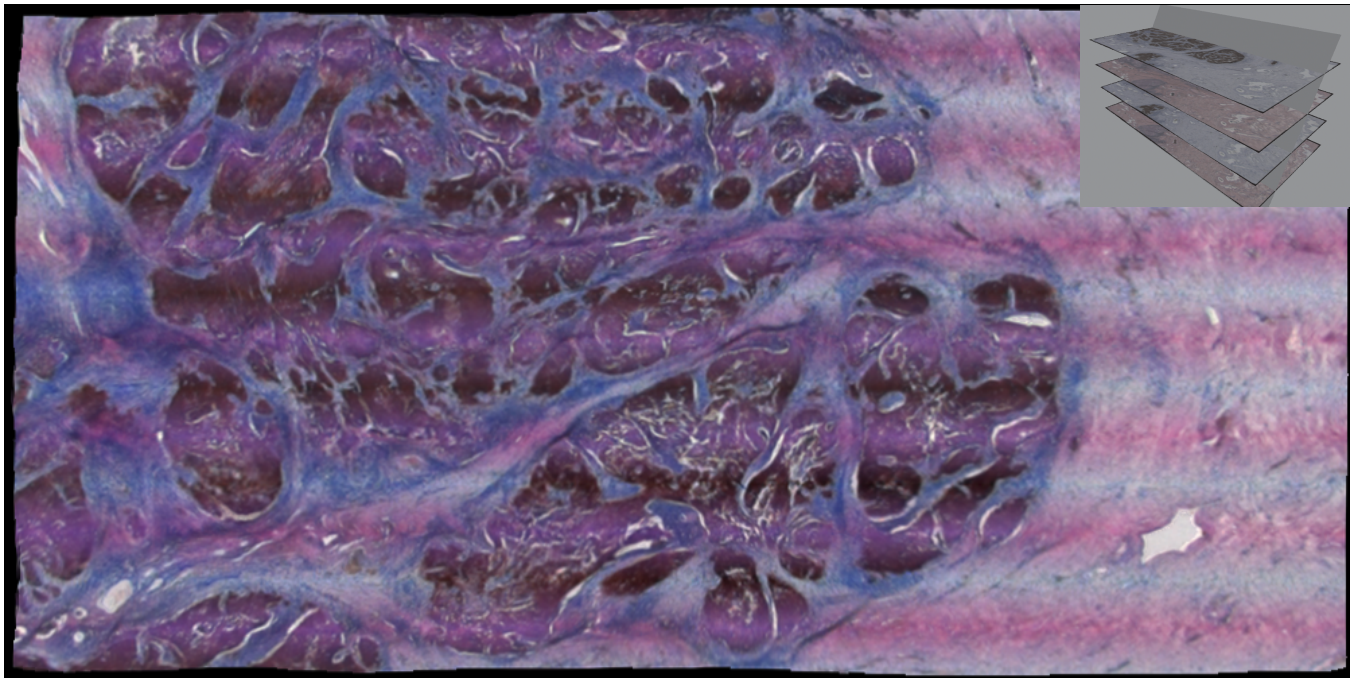

Fig. 4. Illustrative representation of the obtained reconstruction quality for an alternately H&E/p16^{INK4a} stained serial section (with an overall of 350 slices). The oblique plane in the upper right schematic depicts how the virtual cutting plane was basically placed for the *virtual section* shown here. Setting a plane with a tilt angle of 2° about 15 physical slices are traversed. Image extents approximately correspond to 8×4 mm^2 of tissue.

was registered onto the consistent segmentation of its predecessor. The lower part of Figure 4 shows the result of this procedure.

5. CONCLUSIONS AND FUTURE WORK

We have shown a method for the registration of microscopic sections with different stainings on the base of the consistent segmentation of the respective images. The method was successfully applied onto an alternating sequence of H&E/p16^{INK4a} stained images. Our work continues with the application of the newly developed method for other stainings and the registration of serial sections with more than just two different stainings.

6. REFERENCES

[1] Bangalore S. Manjunath, Jens-Rainer Ohm, Vinod V. Vasudevan, and Akio Yamada, "Color and texture descriptors," *IEEE Transactions on Circuits and Systems for Video Technology*, vol. 11, no. 6, pp. 703–715, 2001.

[2] Luca Lucchese and Sanjit K. Mitra, "Color image segmentation: A state-of-the-art survey," *Proceeding of the Indian National Science Academy A (Physical Sciences)*, vol. 67, no. 2, pp. 207–221, 2001.

[3] Bangalore S. Manjunath and Wei-Ying Ma, "Texture features for browsing and retrival of image data," *IEEE Transactions on Pattern Analysis and Machine Intelligence*, vol. 18, no. 10, pp. 837–842, 1996.

[4] Todd K. Moon, "The expectation-maximization algorithm," *IEEE Signal Processing Magazine*, pp. 47–60, 1996.

[5] Franz Pernkopf and Djamel Bouchaffra, "Genetic-based EM algorithm for learning Gaussian mixture models," *IEEE Transactions on Pattern Analysis and Machine Intelligence*, vol. 27, no. 8, pp. 1344–1348, 2005.

[6] Yali Amit, "A nonlinear variational problem for image matching," *SIAM Journal on Scientific Computing*, vol. 15, no. 1, pp. 207–224, Jan. 1994.

[7] Bernd Fischer and Jan Modersitzki, "Curvature based image registration," *Journal of Mathematical Imaging and Vision*, vol. 18, pp. 81–85, Jan. 2003.

[8] Ulf-Dietrich Braumann, Jens-Peer Kuska, Jens Einenkel, Lars-Christian Horn, Markus Löffler, and Michael Höckel, "Three-dimensional reconstruction and quantification of cervical carcinoma invasion fronts from histological serial sections," *IEEE Transactions on Medical Imaging*, vol. 24, no. 10, pp. 1286–1307, Oct. 2005.